

1 Supplementary Materials

2 A preliminary evaluation of the influence of environment- and age-related spatial 3 autocorrelation on the required number of time since last fire sample-points

4 Introduction

5 This supplementary material contextualizes the results of Wei and Larsen (2018) by providing a
6 preliminary evaluation of potential influences of spatial autocorrelation on the number of time since
7 last fire (TSLF) points required to obtain an absolute difference in the measured mean (ADMM) of
8 <10% in the estimate of the fire cycle (FC). Two sources of spatial autocorrelation missing in Wei and
9 Larsen (2018) were those that may occur due to spatial-environmental changes in the hazard of
10 burning [e.g. 1] and those that may occur due to age-related changes in the hazard of burning that
11 occurs in many forest types [e.g. 2]. For example, simulations have shown that age-related increases
12 in the hazard of burning led to high positive spatial autocorrelation in forest ages [3]. In our research,
13 spatial-environmental sources of spatial autocorrelation were missing because we employed a
14 homogenous landscape that had no spatial variations in the hazard of burning. Further, age-related
15 changes in the hazard of burning, that might cause spatial autocorrelation in forest ages [3], could
16 not occur in our study as the stacking of fire-year maps that we employed to create TSLF maps
17 (Section 2.5 of Wei and Larsen 2018) resulted in an equal chance of reburning for all forest ages.

18 Methods

19 We wrote programs in Python to construct and analyze neutral landscapes [4] of forest ages in
20 nine steps. In these landscapes, forest ages represent the TSLFs. A total of 1331 landscape maps were
21 created, each having a unique combination of 11 levels of spatial autocorrelation across 2500 grids,
22 11 levels of spatial autocorrelation of forest ages for 1764 cells within each grid, and 11 levels of
23 age-related changes in hazard of burning (i.e. $11 \times 11 \times 11 = 1331$).

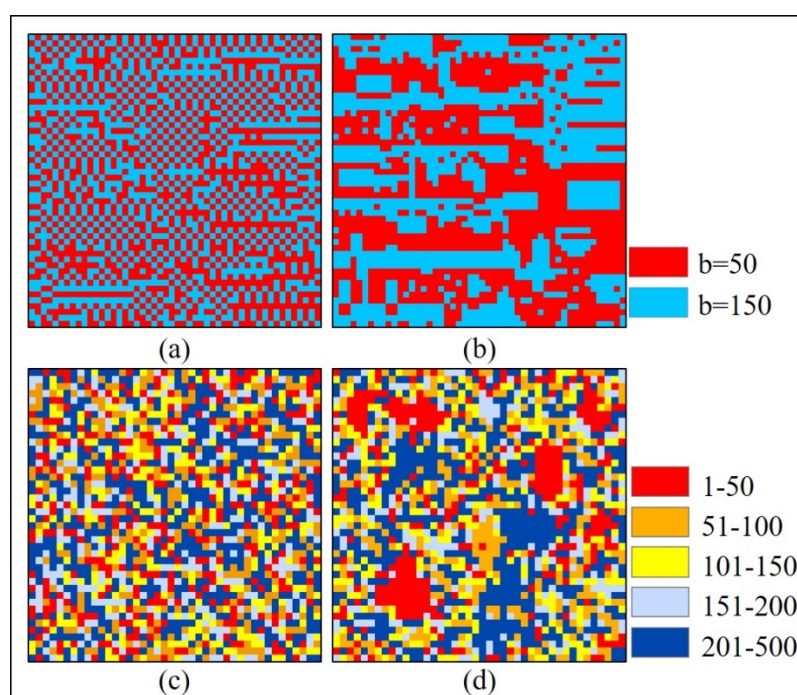
24 First, a landscape of 2100x2100 cells was divided into 2500 non-overlapping square grids that
25 each contained 1764 cells (Figures S1 and S2). The landscape thus had the same dimensions and
26 same number of cells (4,410,000) as the landscape employed in our LANDIS-II simulations (Wei and
27 Larsen, 2018). Second, to represent spatial variation in the hazard of burning, half of the 2500 grids
28 were given a mean fire recurrence (b parameter) of 50 years and half were given a mean fire
29 recurrence of 150 years. Third, random numbers were used to rearrange the 2500 grids into different
30 spatial patterns, the spatial autocorrelation of which was measured using a global Moran's I [5];
31 patterns were selected that represented each of 11 non-overlapping classes 0.2 units wide, from
32 perfectly dispersed (-1), to random (0), to perfectly clustered (1) (Figure S1 a, b).

33 Fourth, the influence of forest age on hazard of burning was assessed by employing 11-levels of
34 c in the Weibull distribution (Equation S1), from 1.0 to 3.0 in increments of 0.2. The c parameter
35 results in age distributions that range from a c of 1 that creates a negative exponential distribution
36 that contains no age-related change in hazard of burning, to a c of 3 that creates an approximate
37 normal distribution that contains strong age-related changes in hazard of burning. Fifth, frequency
38 distributions were created using Equation S1, by employing each of the eleven values of c and both
39 of the levels of mean fire recurrence ($b=50$ year, $b=150$ years). Those frequency distributions were
40 then used in the sixth step to distribute ages across the 1764 cells in each of the 2500 grids.

$$41 \quad f(t) = ct^{c-1}/b^c \exp \left[-\left(\frac{t}{b}\right)^c \right] \quad (S1)$$

42 Sixth, the influence of forest age on hazard of burning was further assessed by employing 11
43 levels of Moran's I (-0.35~-0.25, -0.25~-0.2, -0.2~-0.15, -0.15~-0.08, -0.08~-0.02, -0.02~0.02, 0.02~0.08,
44 0.08~0.15, 0.15~0.2, 0.2~0.25, 0.25~0.35) for the 1764 cells in one grid (Figure S1 c, d). This was done by
45 randomly distributing the forest ages from step five and choosing the first created spatial
46 arrangement of ages that met the required level of global Moran's I. This process was repeated until

47 1250 grids with the required level of Moran's I were created. This process was conducted for both
 48 levels of $b=50$ and $b=150$ years. Thus the 2500 tiles were randomly placed on the neutral landscape
 49 according to the b value. This process was repeated for all the eleven levels of Moran's I under with the
 50 identical spatial pattern and level of c . Seventh, for each neutral landscape model with a given level
 51 of b and c and global Moran's I of ages (Figure S2); the spatial autocorrelation of forest ages in that
 52 neutral landscape was then calculated as the mean of the global Moran's I for a grid with $b=50$ years
 53 and for a grid with $b=150$ years (remember, in each neutral landscape model, all grids with the same
 54 b have the same spatial pattern of forest ages). Eighth, the number of TSLF sample-points required to
 55 estimate the forest age in a neutral landscape model with a ADMM of 10% was calculated as in
 56 section 2.9 of Wei and Larsen (2018). The mean age of the neutral landscape that was assessed in this
 57 step was retained for step nine.



58
 59 **Figure S1.** Examples of the arrangement of the spatial pattern of (a) 2500 grids with a global Moran's
 60 I of -0.6875, (b) 2500 grids with a global Moran's I of 0.7110, (c) 1764 cells with $b=150$, $c=2.0$ and a
 61 global Moran's I of -0.3201, (d) and 1764 cells with $b=150$, $c=2.0$ and a Moran's I of 0.3454. Colors in (a)
 62 and (b) indicate the length of the b parameter in years in the 2500 grids; colors in (c) and (d) indicate
 63 the age in years of each of the 1764 cells.

64 Ninth, stepwise multiple regression was conducted to evaluate the influence of different factors
 65 on the required number of TSLF sample-points. The dependent variable was the 95th percentile of
 66 TSLF points in each of the neutral landscapes; the independent variables were the global Moran's I
 67 of the spatial pattern of b across the 2500 grids, the global Moran's I of the spatial pattern of forest
 68 ages for the 1764 cells within the 2500 grids, the c used for that neutral landscape, and the mean age
 69 of the neutral landscape. Forward-selection and backward-elimination stepwise multiple regression
 70 models were employed with, respectively, p -entering and p -removal values of $p=0.10$.

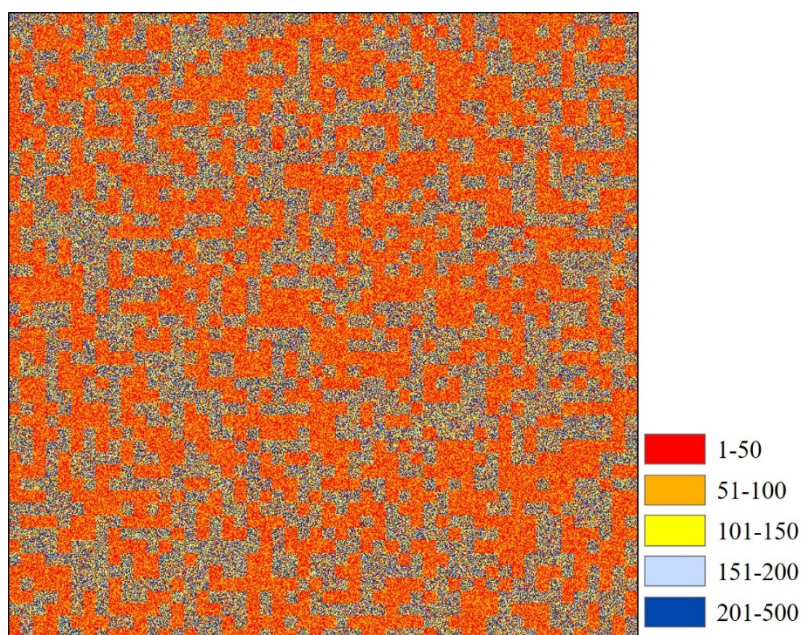


Figure S2. This example of the neutral landscape has a global Moran's I of 0.0854 across the 2500 grids. The mean global Moran's I is 0.0182 for the 1764 cells within the 1250 grids of $b=50$ and 0.0450 for the 1764 cells within the 1250 grids of $b=150$. Colors indicate ages of the 4,410,000 cells.

Results

A total of 1331 neutral landscape maps were created: 11 levels of spatial autocorrelation across the 2500 grids, 11 levels of spatial autocorrelation for the 1764 cells within each of the 2500 grids, and 11 levels of c for forest age frequencies within the grids. The global Moran's I for the spatial pattern of the 2500 grids ranged from -0.970 to 0.969. The global Moran's I for the spatial pattern of forest ages for the 1764 cells within the 2500 grids ranged from -0.319 to 0.344. Values of c ranged from 1.0 to 3.0. Mean cell age of the neutral landscapes ranged from 95.0 to 104.0 years. The 95th percentile of number of samples required for an ADMM of 10% ranged from 206 to 282.

The forward- and backward-selection stepwise regression models returned the same equation to predict the required number of TSLF sample-points (N):

$$N = 240.7 + (10.7 * \text{global Moran's I across grids}) + (73.2 * \text{global Moran's I inside grids}) \quad (S2)$$

The constant and the two slope parameters were all significant ($p=0.0000$), with $R^2_{\text{adj}}=0.861$ ($N=1331$).

Discussion

We found that increased clustering of forest ages within a grid (i.e. higher global Moran's I), and of the b -parameter across grids, required a larger number of TSLF sample-points to accurately estimate the FC. This agrees with theory that shows that study areas with higher spatial autocorrelation require more sample-points to provide a spatially representative estimate of the mean [6]. Higher values of the global Moran's I (i.e. greater clustering) for the 1764 cells of forest age with a grid, is analogous to the increase in local spatial autocorrelation with increased age-related hazard of burning found in simulations [3]. That we did not find any significant relations between the required number of TSLF samples and the value of the c parameter, which creates an age-related change in the hazard of burning, suggests it is not the change in the frequency of forest ages that influences the spatial autocorrelation of forest ages. Instead, changes in the c parameter may only influence the required number of TSLF sample points if those changes influence the spatial autocorrelation of forest ages.

The greater range in global Moran's I that we were able to attain for the 2500 grids than for the 1764 cells within a grid, is likely due to their only being two conditions for the grids ($b=50$ or $b=150$),

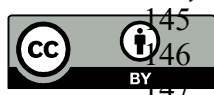
103 while there were hundreds of cell ages within a grid. In a more realistic environment the grids
104 would have a greater variety of values of b due to the continuous variation in environmental drivers
105 of b . Further research is thus required to assess the relative importance of the environmental and age
106 related sources of spatial autocorrelation.

107 It would have been useful to contextualize the range of global Moran's I values obtained from
108 our neutral landscapes with values from field-based or simulated fire histories, but we found none.
109 However, the global Moran's I in the 11 simulated TSLF maps analyzed by Wei and Larsen (2018;
110 sections 2.6 and 3.4) did increase progressively from -0.117 in the TSLF map with a FC of 61 years
111 based on 1200 fire-year maps, to 0.120 for the TSLF map with a FC of 201 years based on 1000
112 fire-year maps. Since a spatially homogenous landscape over which fires would burn randomly was
113 used to build the TSLF maps, we can employ Equation A2 to predict the required number of TSLF
114 sample-points by using a global Moran's I across grids value of zero. The model then predicts that
115 232 TSLF sample-points would be required for the negatively spatially autocorrelated TSLF map
116 based on 1200 fire-year maps, and that 250 TSLF sample-points would be required for the positively
117 spatial autocorrelated TSLF map based on 1000 fire-year maps. These values are slightly lower than
118 the 267 TSLF points that our dynamic simulations created using LANDIS-II indicated would be
119 needed for this 6X scale landscape (Wei and Larsen, 2018). However, the non-significant Spearman
120 rank correlation ($r_s=-0.092$, $p=0.789$, $N=11$) between global Moran's I and the 95th percentile of the
121 number of TSLF points required to estimate the FC with an ADMM <10% (Wei and Larsen 2018,
122 section 3.4) suggest that these variations in global Moran's I did not influence the required sample
123 size in our TSLF maps.

124 This preliminary evaluation thus does indicate that spatial- and age-related variations in the
125 hazard of burning would influence the required number of TSLF sample-points. However, these
126 neutral landscape models were not developed using dynamic properties related to the spread of
127 fires, nor empirical relations between forest age and the hazard of burning, nor realistic spatial
128 patterns in how the hazard of burning varies across a landscape. Our results are thus not applicable
129 in field settings, but are suggestive of the potential influence of these factors on the required number
130 of TSLF sample-points.

131 References

- 132 1. Larsen, C.P.S. Spatial and temporal variations in boreal forest fire frequency in northern Alberta. *Journal of*
133 *Biogeography* **1997**, *24*, 663-673.
- 134 2. Price, O.F.; Pausas, J.G.; Govender, N.; Flannigan, M.; Fernandes, P.M.; Brooks, M.L.; Bird, R.B. Global
135 patterns in fire leverage: the response of annual area burnt to previous fire. *International Journal of Wildland*
136 *Fire* **2015**, *24*, 297-306.
- 137 3. Kitzberger, T.; Araoz, E.; Gowda, J.R.; Mermoz, M.; Morales, J.M. Decreases in fire spread probability with
138 forest age promotes alternative community states, reduced resilience to climate variability and large fire
139 regime shifts. *Ecosystems* **2012**, *15*, 97-112.
- 140 4. Gardner, R.H.; Milne, B.T.; Turner, M.G.; O'Neill, R.V. Neutral models for the analysis of broad-scale
141 landscape pattern. *Landscape Ecology* **1987**, *1*, 19-28.
- 142 5. Moran, P.A.P. Notes on continuous stochastic phenomena. *Biometrika* **1950**, *37*, 17-23.
- 143 6. Griffith, D.A. Effective geographic sample size in the presence of spatial autocorrelation. *Annals of the*
144 *Association of American Geographers* **2005**, *95*, 740-760.



© 2018 by the authors. Submitted for possible open access publication under the terms and conditions of the Creative Commons Attribution (CC BY) license (<http://creativecommons.org/licenses/by/4.0/>).